JOURNAL OF MATERIALS SCIENCE 29 (1994) 5765–5772

Optical, mechanical and water drop impact characteristics of polycrystalline GaP

J. M. WAHL, R. W. TUSTISON
Raytheon Co., Research Division, Lexington, MA 02173, USA

A polycrystalline form of GaP has been synthesized and its optical and mechanical properties determined. The optical transmission is found to be intrinsic at long wavelengths in the infrared, being limited only by Fresnel reflection and multiphonon absorptions, beginning at approximately 1100 cm^{-1}. The optical cut-off at short wavelengths is in agreement with earlier measurements on single crystal material. The fracture toughness of the polycrystalline material is found to be greater than that previously reported for single-crystal material. The single impact water drop damage velocity threshold (2 mm drop diameter) was estimated to be 250–280 $m\,s^{-1}$, which is consistent with the measured polycrystalline fracture toughness.

1. Introduction

Optical imaging systems operating at long wavelengths in the infrared (LWIR) portion of the spectrum, i.e. 8–12 μm, require materials from which various optical components can be manufactured. Of primary importance is the degree of transparency. Stability and durability are also important in those applications where the optical material comprises the exterior element of a system expected to operate in a hostile environment, e.g. high-speed liquid drop impact.

The search for a truly durable, multispectral LWIR transparent material has been long and generally unsuccessful. With few exceptions, materials which transmit beyond 8 μm in wavelength tend to be soft, weak or in the worse case water-soluble. For example, the alkali-halides that have served as ideal wide band-pass windows in laboratory equipment are of no practical use as external windows. At the other extreme, crystalline diamond, while perhaps acceptable for small windows, is not likely to be utilized for very large windows in the immediate future although recent advances in vapour phase deposition of crystalline diamond have stimulated interest in this application. Between these ideals there exists a variety of compromise materials from which to choose, depending on the specific application. For example, materials like ZnS, ZnSe and Ge have been developed and are being used while other II–VI and III–V semiconducting compounds have been suggested as potentially useful [1]. Of the latter group, gallium phosphide (GaP) has perhaps the most interesting set of physical and optical properties, being relatively hard with broadband transparency. Its combination of high thermal conductivity and low coefficient of thermal expansion also implies good resistance to thermal shock [2].

Unfortunately, the optical and physical properties of GaP reported to date have been for single-crystal or very large-grain material. It is expected that grain size will affect mechanical properties. For example, it is well known that semiconducting single crystals having the zinc blende structure (e.g. GaAs, GaP) cleave most readily along (1 1 0) planes, where charge neutrality is preserved, and not as readily between (1 0 0) and (1 1 1) planes. By contrast, single crystal semiconductors of the diamond-type crystal structure (e.g. Si, Ge) cleave most readily along (1 1 1) planes. This cleavage behaviour is reflected in markedly lower fracture toughness values associated with the characteristic cleavage plane [3, 4].

Fracture toughness has been proposed as an indicator of resistance to water drop impact induced damage [5]. For large-grain or single-crystal material, high-velocity water drop impact results in preferential fracture along cleavage planes. As the grain size is decreased below the contact radius of the liquid drop (which is approximately 0.2 mm for 2.0 mm diameter drops impacting at velocities below 400 $m\,s^{-1}$) the tendency for cleavage decreases and more typical polycrystalline damage behaviour is observed.

Indentation hardness has also been found to increase with decreasing grain size [6]. Therefore the mechanical and optical properties of fine grain GaP are of interest. We report here selected optical, mechanical and water drop impact damage characteristics of polycrystalline GaP.

2. Experimental procedure

2.1. Optical measurements

Polycrystalline samples of GaP were grown by an open-tube, chemical vapour deposition process, utilizing a halogen (chlorine) as the transporting agent. The Ga–PCl_3–H_2 system has been described extensively, both experimentally [7–9] and analytically [10–12]. Thirty-seven deposition experiments were carried out, yielding sufficient material for evaluation.

0022–2461

The surface of the deposited GaP presents an angular hillock growth structure. X-ray diffraction analysis indicated no preferred growth direction. Optical micrographs of this surface as well as a typical cross-section of the material following polishing are shown in Fig. 1a and b, respectively. The grain structure was revealed by etching for 5 s in a solution of $K_3Fe(CN)_6$–KOH–H_2O. The average grain diameter is approximately 50 μm, but varies with the thickness of the deposit which is typical of chemically vapour-deposited material, e.g. ZnSe.

Samples in the shape of disks were ground and polished on both surfaces and optical transmission measurements were performed using a 580B Perkin Elmer grating spectrophotometer as well as an FT-IR Bomem MB120 spectrophotometer equipped with a 4x microbeam.

2.2. Mechanical measurements

Samples of GaP were fabricated into the shape of bars, approximately 28.6 mm in length, and the linear thermal expansion coefficient was determined over the range of room temperature to 500 °C using a Unitherm 2000 dilatometer. The changes in sample length were measured upon heating as linear displacements on a transducer to a sensitivity of 1 μm. A linear heating rate of 2.0 °C min^{-1} was used. The results for GaP are summarized in Table I.

Microhardness measurements were made using a Kentron microhardness indenter with a Knoop-geometry, diamond stylus. Thirty indentations at 50 g load were typically taken and the results averaged to obtain a microhardness number.

A Vickers pyramid indenter was exchanged with the Knoop indenter and the Vickers hardness number as well as the indentation fracture toughness was determined as a function of applied load for both GaP and ZnS.

2.3. Water drop impact testing

The effects of high-velocity, single water drop impact were simulated using an impact jet apparatus. The calibration and use of this instrument has been discussed extensively elsewhere [13]. A 0.8 mm diameter nozzle was used to form the jet over a series of jet velocities ranging from approximately 200 to 300 m s^{-1}. GaP samples, 1 mm in thickness, were ground and polished in the shape of disks, approximately 1 mm thick. These samples in turn were glued to the surfaces of 6 mm thick, ZnS samples which provided support for the thinner GaP during impact. ZnS samples alone were also impacted for the sake of comparison.

In addition to single-impact experiments, multiple-impact tests were performed by the University of Dayton Research Institute at the rotating arm facility

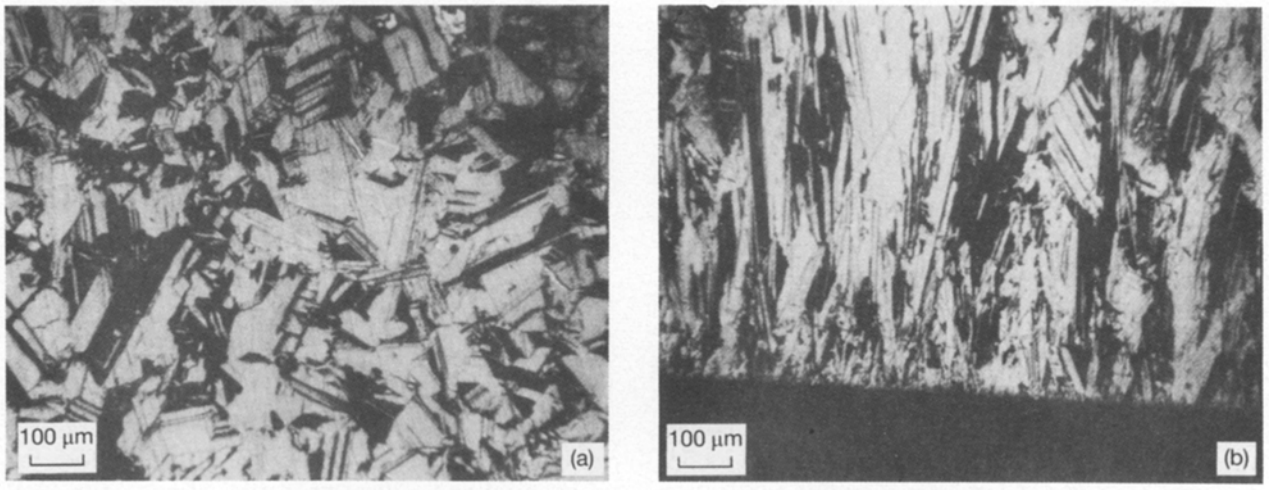

Figure 1 Microstructure of chemically vapour-deposited GaP in plane view (a) and in cross-section (b).

TABLE I Physical properties of LWIR materials

Property	GaP	GaAs	ZnSe	ZnS	$CaLa_2S_4$	Ge	Si	C
Crystal structure	zb	zb	zb	zb	sp	d	d	d
Density ($g\,cm^{-3}$)	4.13	5.32	5.27	4.08	4.26	5.32	2.33	3.5
Young's modulus (GPa)	143	108	68	75	96	104	132	–
Thermal expansion coefficient ($10^{-6}\,°C^{-1}$)	5.3	6.5	7.6	7.8	14.7	6.1	2.8	1.8
Flexural strength (MPa)	–	76	52	103	106	90	–	–
Knoop hardness ($kg\,mm^{-2}$) 50 g load	834	630	100	250	570	690	1150	10000
Fracture toughness ($MPa\,m^{-1/2}$)	1.1	0.43	0.78 0.90	1.1	0.53	0.66	0.95	–

zb – zincblende; ch – chalcopyrite; d – diamond; sp – spinel.

in Dayton, Ohio [14]. For these tests, 2.22 cm diameter disks were fabricated and exposed in a 2.54 cm h^{-1} simulated rain field of 2.0 mm diameter drops, 90° impact angle. The duration of the exposure as well as the sample velocity were the experimental variables.

3. Results and discussion

3.1. Optical properties

Fig. 2 shows the transmittance as a function of wavelength for a 1 mm thick sample of polycrystalline GaP. The long wavelength transmittance cut-off, defined by the onset of multiphonon lattice modes, clearly begins in the vicinity of 11.1 μm and is essentially complete at 13.5 μm. The transmittance level reaches a maximum in the LWIR of approximately 62%, consistent with a Fresnel limit calculated from the refractive indices given by Ref. 2 ($n_{avg} = 2.895$).

Of particular interest is the origin of the absorption band(s) in the vicinity of 9 μm. Fig. 3 shows an expanded view of this region, obtained on the Bomem FT-IR spectrophotometer. One can see that this absorption feature is actually the superposition of three distinct bands, occurring at 8.8 (1136 cm^{-1}), 9.1 (1099 cm^{-1}) and 9.3 (1075 cm^{-1}) μm respectively, with additional bands occurring beyond 10 μm, most notably at 10.9 (917 cm^{-1}) μm.

Klocek *et al.* [2] observed a large absorption band at 1100 cm^{-1} in their liquid-encapsulated (boric oxide glass), Czochralski single-crystal GaP. They attributed this absorption to a combination of intrinsic phonon and extrinsic impurity molecular vibration modes. Barker *et al.* [15] conducted a study of localized vibrational modes in GaP, primarily looking for oxygen impurities. They intentionally doped GaP with Ga_2O_3 and observed a line at 1002 cm^{-1} and several weaker lines in the region up to 1150 cm^{-1}. They concluded that interstitial oxygen contributed an absorption in LEC grown crystals encapsulated with B_2O_3 at 1002 cm^{-1} but the three-peaked absorption feature above 1000 cm^{-1} was attributed to a three-phonon process. Measurements made by Ulrici *et al.* [16] on V-, Cr- and Ti-doped GaP seemed to confirm the earlier assignments by Barker.

In the present work the microcrystalline GaP was deposited in a reducing atmosphere and therefore contained no detectable oxygen. Using the data of Fig. 3 Klein [17] has made preliminary assignments of all the primary absorption features, in particular assigning the 8.8 (1136 cm^{-1}) and 9.3 (1075 cm^{-1}) μm features to 3-LO and 3-TO harmonics, respectively. The remainder of the features were successfully related to combination TO, LO and LA modes. In particular, the strong absorption feature observed in LEC material at 1002 cm^{-1} and attributed by Barker *et al.* to interstitial oxygen is not observed in the chemically vapour-deposited material of the present investigation. This implies that the observed transmittance is representative of intrinsic, multiphonon behaviour.

Kleinman and Spitzer [18] have reported the room-temperature, short-wavelength cut-off of GaP to be at 0.55 μm wavelength or 2.24 eV. This is also in agreement with the data shown in Fig. 2. Where this data differs from that obtained on single-crystalline GaP is reflected in the observed dependence of the transmittance on the wavelength beyond 0.55 μm.

It is believed that the decrease in transmittance at shorter wavelengths is caused by dislocations at the grain boundaries. This is shown in Fig. 4, which is a micrograph of a grain boundary region taken with transmitted light. The grain boundaries are clearly shown as high contrast areas. Also note the appearance of slip lines along the grain boundaries, also shown in contrast. Slip lines or bands have been observed previously in single-crystal GaP by both Boehnke *et al.* [19] and Hilgarth [20] using optical microscopy. DeKoch *et al.* [21] observed slip lines in Czochralski-grown single crystals emanating from the crystal surface. The slip lines evident in Fig. 4 are also reminiscent of those observed in Type I diamond [22]. The stress which produced these slip lines must occur following completion of the deposition and while the GaP material is separating from the vitreous carbon substrate. Evidently this occurs at temperatures which are still in excess of the 500–600 °C required for significant plasticity to occur in GaP [23, 24].

Dislocations associated with these slip bands and grain boundary regions also affect the electrical properties of polycrystalline GaP. The carrier type and

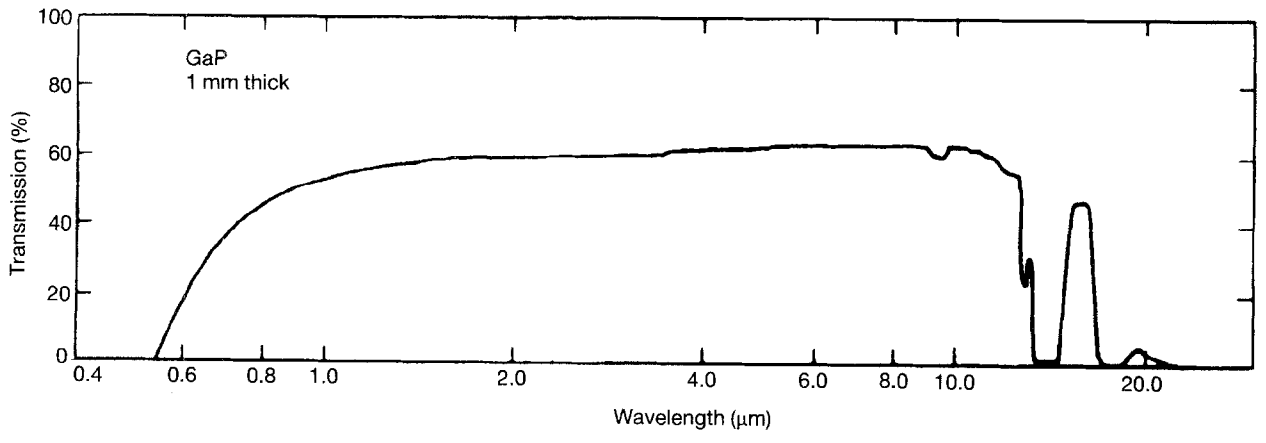

Figure 2 Transmittance as a function of wavelength for a 1 mm thick sample of GaP.

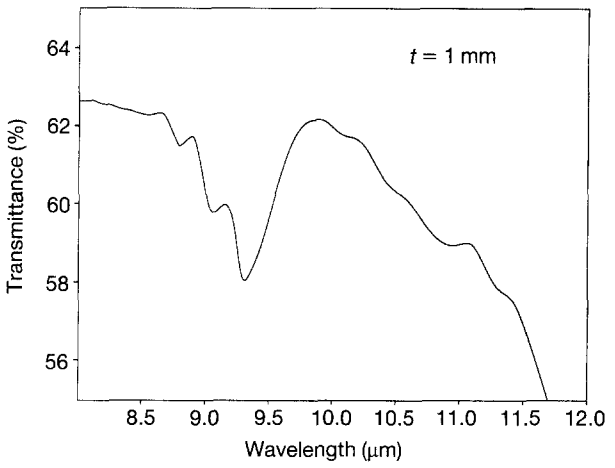

Figure 3 Long wavelength transmittance of a 1 mm thick sample of GaP.

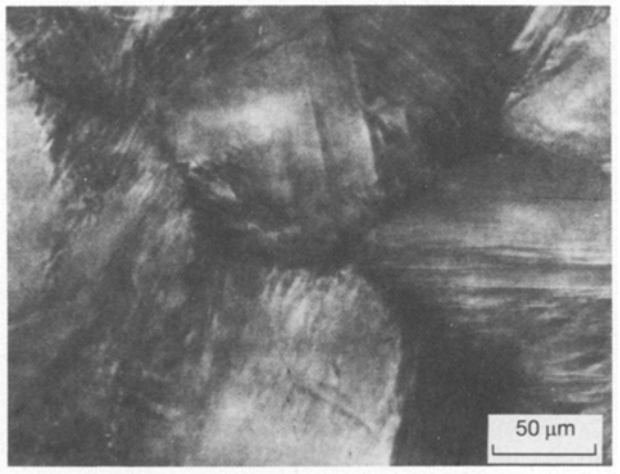

Figure 4 Optical micrograph of the grain boundary region of chemically vapour-deposited GaP taken in transmitted light.

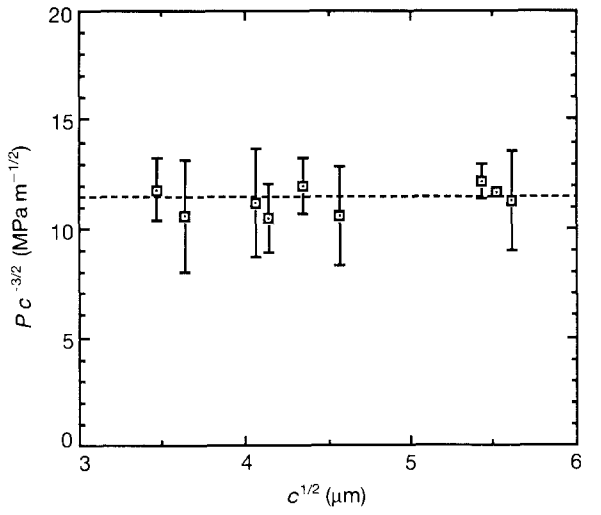

Figure 5 Indentation load (P) divided by the half-penny crack length to the three halves power ($c^{3/2}$) as a function of $c^{1/2}$. Note the invariance of the load to crack length ratio on crack length.

concentration were determined by Van der Pauw Hall measurement. Single-crystal GaP is generally reported to be n-type with carrier concentrations ranging from 10^{15} to 10^{18} cm^{-3} and mobilities of 80–140 cm^2 V-s^{-1}. The polycrystalline material of the present investigation was also n-type with a relatively low carrier concentration of 9.3×10^9 cm^{-3} and mobility of 3 m^2 V s^{-1}. The resistivity was found to be 2.5×10^8 Ω cm. Dislocations are known to reduce both carrier concentrations and their mobility in n-type semiconductors [19], and that appears to be the case here.

3.2. Mechanical properties

The microhardness and fracture toughness of microcrystalline GaP was also determined. Fracture toughness is an important material parameter in the sense that it is related to the ultimate fracture strength as has been discussed by Mecholsky [25]. Fracture toughness has also been proposed as an indicator of resistance to raindrop-induced damage [5].

The fracture toughness parameter (K_c) determination was based on the formation in the material of a half-penny crack which is created as a result of the residual contact stress field around a Vickers indentation [26–28]. Indentations were made over the load (P) range of 0.05–0.20 kg for GaP and 0.40–1.0 kg for ZnS. The lower load limit was established by the requirement [26] that the crack length c be greater than or equal to twice the indent diagonal a. The upper load limit was set by the maximum load obtainable without chipping around the indent. Indentations were made in air, with a residence hold time of 15 s, and the sample was allowed to equilibrate for at least 24 h before measurement to ensure that stress-induced slow crack growth of the radial cracks had ceased [27]. A test of the validity of the indentation measurement of the fracture toughness is a demonstration of the invariance of the ratio $Pc^{-3/2}$ to the crack size c.

For an indentation load P the radius c of the surface half-penny crack is determined from the residual stress intensity factor associated with the residual contact field

$$K_c = XP(c)^{-3/2} \quad (1)$$

where X is a dimensionless field intensity parameter [28]. At equilibrium, where the crack growth rate (i.e. environmentally assisted rate) is zero, Equation 1 may be rearranged to read

$$Pc^{-3/2} = K_c/X = \text{constant} \quad (2)$$

Therefore a test of the indentation theory is that $Pc^{-3/2}$ should be crack-size invariant. This is demonstrated in Fig. 5. The fracture toughness, measured for GaP and ZnS over a range of loads, is shown in Fig. 6a and b.

Table I summarizes the fracture toughness and Knoop hardness data for GaP and ZnS along with additional thermal and mechanical properties of other LWIR optical materials.

3.3. Water drop impact characteristics

The term *rain erosion* is in some ways a misnomer when applied to the water drop impact damage commonly observed in LWIR transparent materials. Frequently, little if any material is actually removed before

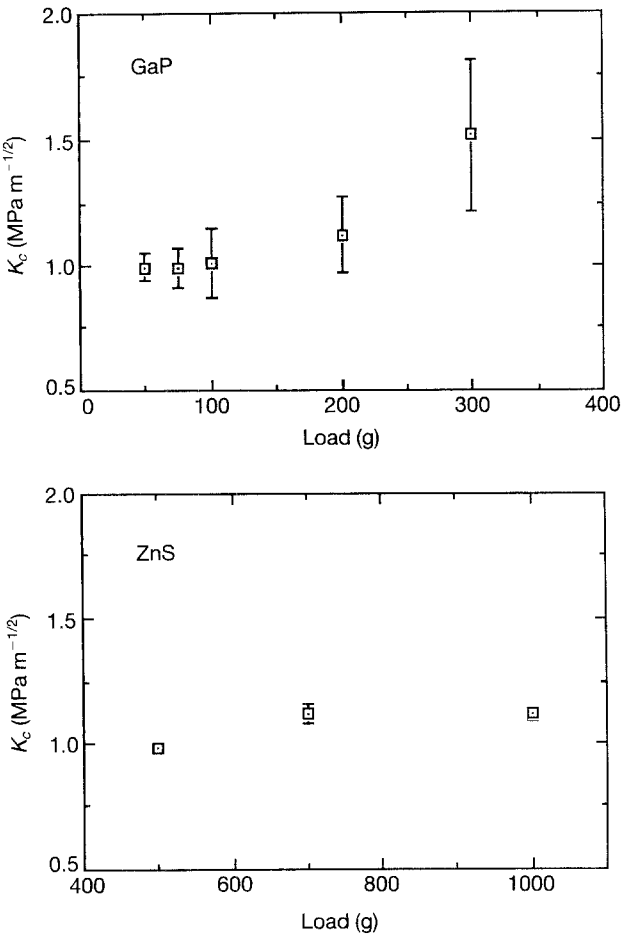

Figure 6 Indentation fracture toughness of GaP (upper) and ZnS (lower) as a function of indenter load. The load was limited by the occurrence of chipping, particularly in the case of GaP which led to uncertainty at the highest load.

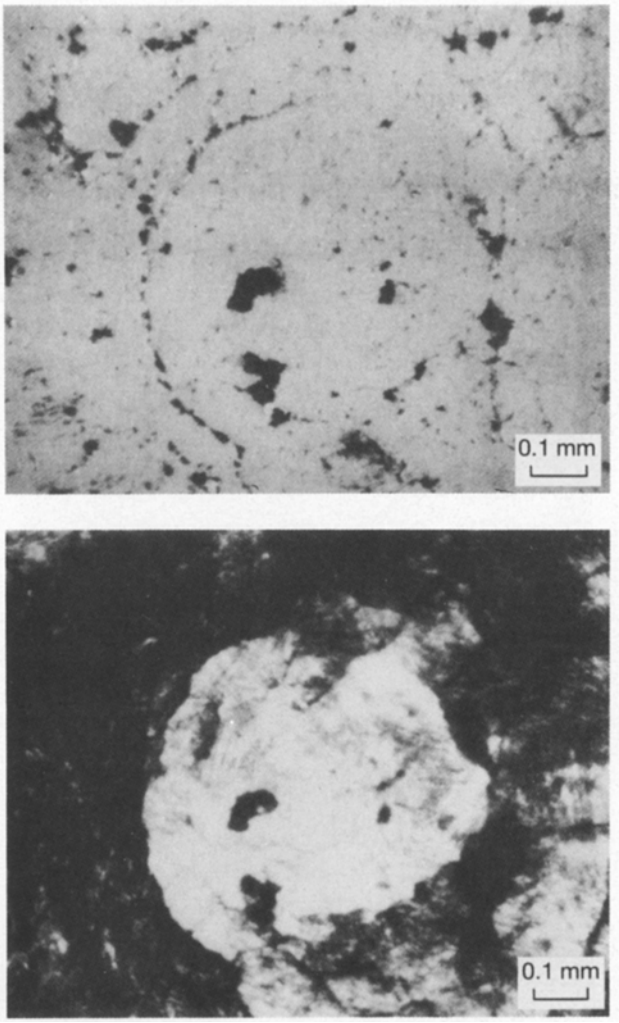

Figure 7 Typical ring fracture in GaP taken in reflected (a) and transmitted (b) light. The sample had been exposed for 5 min at 268 m s^{-1}, 2.54 cm h^{-1} simulated rain field, 2 mm diameter drops.

the sample has suffered substantial, subsurface damage. The fracture pattern observed in microcrystalline GaP following exposure for 5 min at 268 m s^{-1} is shown in Fig. 7. The so-called ring cracks, which are a collection of circumferential cracks, occur in the elastic response regime of the material and are a result of the interaction of preexistent microflaws with the radial tensile component of the Rayleigh wave that propagates from the centre of the impact site [29, 30]. These micrographs were taken both with reflected (a) and transmitted (b) light, the latter showing the central, largely undamaged area, surrounded by a heavily damaged region which includes subsurface fractures which lead to scattering. Also evident in the micrograph is the beginning of surface erosion.

The response of the polycrystalline GaP to single drop impact was also simulated using the water jet apparatus. Jet velocities were varied from 203 to 302 m s^{-1} which corresponds to equivalent 2 mm diameter drop velocities [13] ranging from 280 to 393 m s^{-1} respectively. While the grain structure makes observation difficult, circumferential cracks were first observed at jet velocities of 203 m s^{-1} (280 m s^{-1} equivalent 2 mm drop velocities) as shown in Fig. 8. By comparison, complete ring fractures are clearly formed at the same impact velocities in polycrystalline ZnS as shown in Fig. 9.

Various methods have been suggested to quantify the amount of damage sustained by brittle materials during water drop impact. From an engineering viewpoint, decrease in transmittance of LWIR transparent materials following exposure would be a convenient measure of the onset of damage. This decrease might be measured over the relevant bandpass of interest, e.g. 8–12 μm. In fact, specifications have been written which place limits on the amount of allowable transmittance degradation for a fixed exposure condition. However, significant amounts of damage usually occur before transmittance degradation becomes significant.

Alternatively, Van der Zwaag and Field [31] have suggested that the decrease in fracture strength that accompanies the onset of visible damage is a sensitive indicator of the damage threshold in LWIR materials. They define this after-exposure strength as residual strength and have used it to establish the damage threshold velocity (DTV), namely the water drop impact velocity at which the residual strength decreases below the unexposed value. The microscopic observation of damage sites and their corresponding "ring fractures" has also been used to identify the onset or threshold for damage [32].

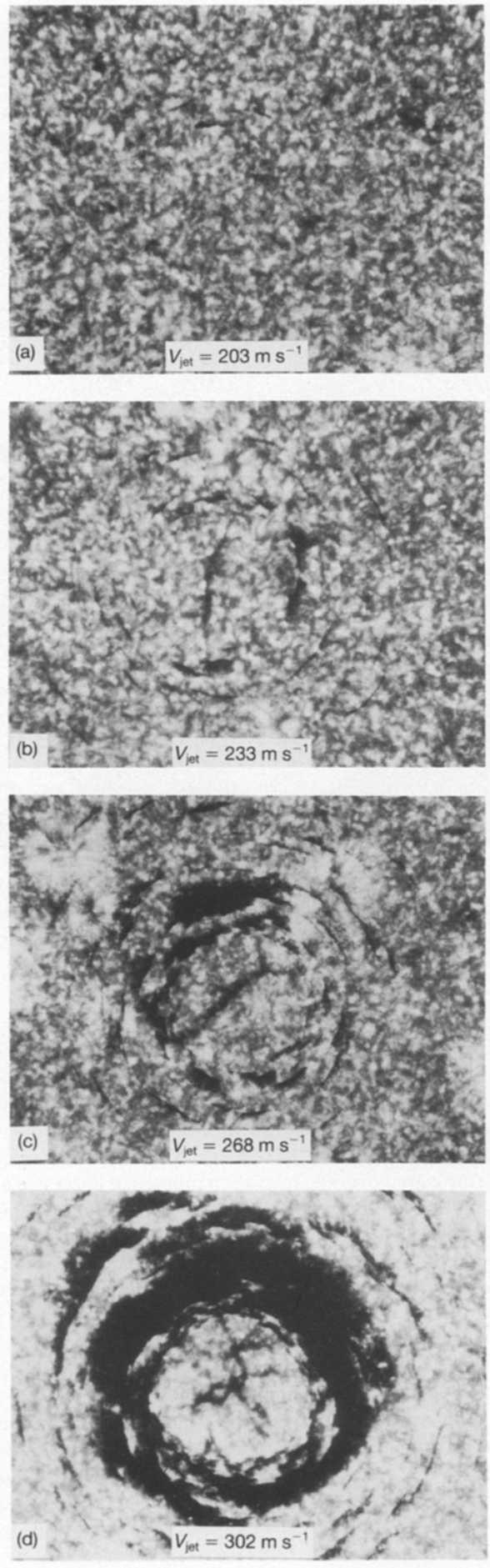

Figure 8 Single water jet impact sites in GaP created at jet velocities [11] of 203, 233, 268 and 302 m s^{-1} which corresponds to equivalent drop velocities of 280, 319, 354 and 393 m s^{-1} respectively for 2 mm diameter drops.

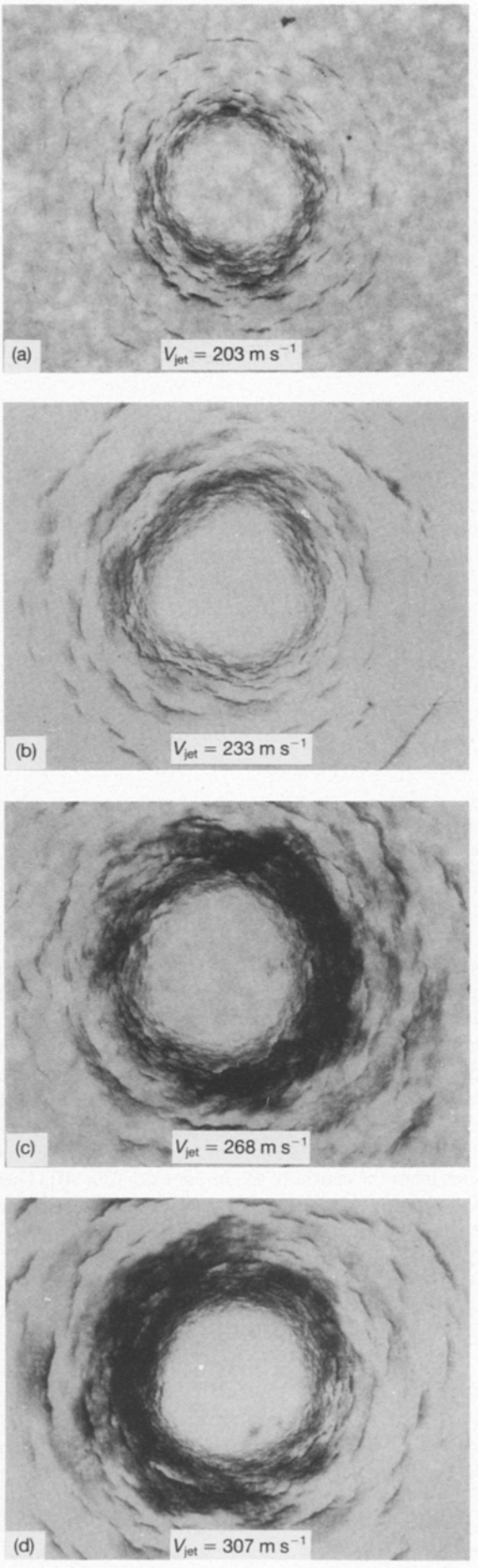

Figure 9 Single water jet impact sites in ZnS created at jet velocities [11] of 203, 233, 268 and 307 m s^{-1} which corresponds to equivalent drop velocities of 280, 319, 354 and 399 m s^{-1} respectively for 2 mm diameter drops.

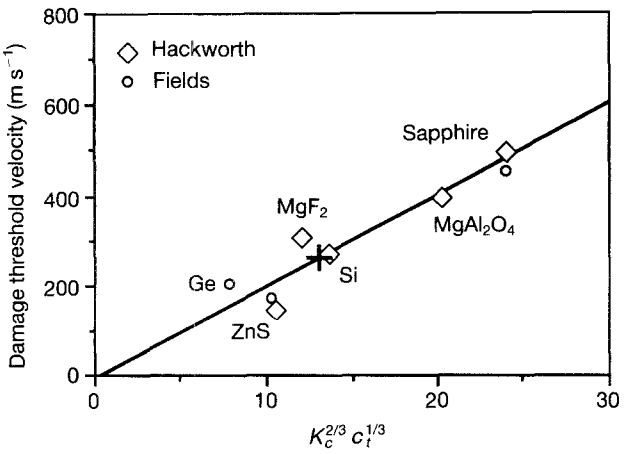

Figure 10 Single impact, damage threshold velocities (DTV) as a function of the "damage parameter" defined as the product $(K_c^{2/3} c_t^{1/3})$ for several long wavelength transparent optical materials.

Evans has suggested [30] that the damage threshold velocity, v_t should be proportional to the fracture toughness K_c and the elastic wave velocity c_t (= modulus/density)$^{1/2}$, namely the product $(K_c^{2/3} c_t^{1/3})$. As a test of this proposal, the single-drop (2.0 mm) data collected by Hackworth and Kocher [33] and by Field [34] was plotted in Fig. 10 against the damage parameter as defined by Evans. The single-drop damage threshold velocity is found to be approximately proportional to the damage parameter over the range of velocities and materials evaluated.

For the present investigation, utilizing an average fracture toughness obtained in Fig. 6 (Table I) for polycrystalline GaP, one can estimate a damage threshold velocity from the curve of Fig. 10 of $270 \pm 20\ m\,s^{-1}$. This is in good agreement with the recent data of Waddell and Monachan [35] who reported a DTV of $250\ m\,s^{-1}$, presumably for large-grain or single-crystal material and also consistent with the onset of circumferential cracking observed at $\sim 280\ m\,s^{-1}$ (2 mm diameter drop) shown in Fig. 8.

4. Summary

Polycrystalline GaP has been synthesized and the mechanical and optical properties of the material determined. The optical transmittance reaches the Fresnel limit in the middle and long wavelength infrared. The short wavelength cutoff occurs at 2.24 eV (0.55 μm wavelength) and is consistent with single-crystal data. However, scattering at shorter wavelengths limits the transmittance in the near infrared-visible and is associated with dislocations at the grain boundaries in the material. Absorption bands occurring between $917\ cm^{-1}$ (10.9 μm wavelength) and $1136\ cm^{-1}$ (8.8 μm wavelength) are intrinsic and associated with three-phonon processes. These phonon processes lead to absorption in GaP which is on average about 3 times stronger than that in ZnS between 8 and 12 μm wavelength. This may eliminate GaP from consideration for some LWIR window applications, particularly at elevated temperatures. However, recent work on polycrystalline GaP films indicates that this material may be very useful for LWIR protective coating applications, where free standing thicknesses are not required [36].

Microhardness and fracture toughness are higher than previously reported for single-crystal GaP. The single liquid drop (2 mm diameter) impact damage threshold velocity is estimated to be $270\ m\,s^{-1}$, based on the measured fracture toughness as well as a damage parameter proposed by Evans. This value is consistent with a previous report by Waddell and Monachan and is greater than the accepted DTV of $175\ m\,s^{-1}$ for chemically vapour-deposited, polycrystalline ZnS but slightly less than the DTV of $274\ m\,s^{-1}$ reported by Hackworth and Kocher [31] for single-crystal silicon.

Acknowledgements

The authors would like to thank J. Pollano for the preparation of the GaP samples, P. Roman for thermal mechanical measurements, T. Varitimos for optical measurements, J. Rawson for single impact water jet tests and H. Hendricks for Hall mobility measurements. Special thanks are extended to Dr P. Miles for his encouragement and enthusiasm during the first phase of this work. The work was sponsored in part by the Materials Laboratory of the Wright Research and Development Center, Wright-Patterson AFB, Dayton, Ohio.

References

1. J. A. SAVAGE, "Infrared Optical Materials and their Antireflection Coatings" (Adam Hilger, Bristol, 1985).
2. P. KLOCEK, L. E. STONE, M. W. BOUCHER and C. DEMILO, in Proceedings of the Society of Photo-Optical Instrumentation Engineers, vol. 929, Infrared Optical Materials VI, edited by S. Musikant (Bellingham, Washington, 1988) p. 65.
3. K. HAYASHI, M. ASHIZUKA, R. C. BRADT and H. HIRANO, *Mater. Lett.* **1** (1982) 116.
4. C. P. CHEN and M. H. LEIPOLD, *Bull. Am. Ceram. Soc.* **59** (1980) 469.
5. A. G. EVANS, *J. Appl. Phys.* **49** (1978) 3304.
6. D. TOWNSEND and J. E. FIELD, *J. Mater. Sci.* **25** (1990) 1347.
7. W. G. OLDHAM, *J. App. Phys.* **36** (1965) 2887.
8. G. S. KAMATH and D. BOWMAN, *J. Electrochem. Soc.* **114** (1967) 193.
9. A. USUI and K. MORI, *Jpn. J. App. Phys.* **15** (1976) 2245.
10. P. KLIMA, J. SILHAVY, V. RERABEK, I. BRAUN, C. CERNY, P. VONKA and R. HOLUB, *J. Cryst. Growth* **32** (1976) 279.
11. H. SEKI and H. ARAKI, *Jpn. J. App. Phys.* **6** (1967) 1414.
12. G.-Q. YAO, H.-S. SHEN, R. KERSHAW, K. DWIGHT and A. WOLD, *Mat. Res. Bull.* **21** (1986) 653.
13. C. R. SEWARD, C. S. PICKLES and J. E. FIELD, Proceedings of the Society of Photo-Optical Instrumentation Engineers, vol. 1326, Window and Dome Materials II, edited by P. Klocek (Bellingham, Washington, 1990) p. 280.
14. J. R. KOLEK Jr, "Wright Laboratory Rain Erosion Test Apparatus Utilization Policies, Operating Procedures and Specimen Configuration – Revision 3" (University of Dayton Research Institute, Dayton OH, 1991).
15. A. S. BARKER, R. BERMAN and H. W. VERLEUR, *J. Phys. Chem. Solids* **34** (1973) 123.
16. B. ULRICI, R. STEDMAN and W. ULRICI, *Phys. Status Solidi* (b) **143** (1987) K135.
17. C. KLEIN, Raytheon Co., personal communications.

18. D. A. KLEINMAN and W. G. SPITZER, *Phys. Rev.* **118** (1960) 110.
19. O. BOEHNKE, E. NOWAK, P. PAUFLER and H. NEUMANN, *Phys. Status Solidi* (a) **75** (1983) K137.
20. J. HILGARTH, *J. Mater. Sci.* **13** (1978) 2697.
21. A. J. R. DEKOCK, W. M. VAN DE WIGERT, J. H. T. HENGST, P. J. ROKSNOER and J. M. P. L. HUYBREGTS, *J. Cryst. Growth* **41** (1977) 13.
22. J. WILKS and E. WILKS, "Properties and Applications of Diamond" (Butterworth–Heinemann, Oxford, 1991) p. 157.
23. I. YONENAGA and K. SUMINO, *J. Mater. Res.* **4** (1989) 355.
24. K. MAEDA, O. UEDA, Y. MURAYAMA and K. SAKAMOTO, *J. Phys. Chem. Solids* **38** (1977) 1173.
25. J. J. MECHOLSKY, S. W. FREIMAN and R. W. RICE, *J. Mater. Sci.* **11** (1976) 1310.
26. G. R. ANTSIS, P. CHANTIKUL, B. R. LAWN and D. B. MARSHALL, *J. Amer. Ceram. Soc.* **64** (1981) 533.
27. B. R. LAWN, K. JAKUS and A. C. GONZALEZ, *ibid.* **68** (1985) 25.
28. B. R. LAWN, A. G. EVANS and D. B. MARSHALL, *ibid.* **63** (1980) 574.
29. W. F. ADLER, *J. Mater. Sci.* **12** (1977) 1253.
30. A. G. EVANS, Y. M. ITO and M. ROSENBLATT, *J. Appl. Phys.* **51** (1980) 2473.
31. S. VAN DER ZWAAG and J. E. FIELD, *J. Mater. Sci.* **17** (1982) 2625.
32. R. W. TUSTISON and R. L. GENTILMAN, Proceedings of the Society of Photo-Optical Instrumentation Engineers, vol. 968, Ceramics and Inorganic Crystals for Optics, Electro-Optics, and Nonlinear Conversion (Bellingham, Washington, 1988) p. 25.
33. J. V. HACKWORTH and L. H. KOCHER, "Final Report No. AFML-TR-78-184" (Bell Aerospace, Buffalo, NY, 1978).
34. J. E. FIELD, S. VAN DER ZWAAG, D. TOWNSEND and J. P. DEAR, "Final Report No. AFWAL-TR-83-4101" (Cavendish Laboratory, Cambridge, UK, 1983).
35. E. M. WADDELL and B. C. MONACHAN, Proceedings of the Society of Photo-Optical Instrumentation Engineers, vol. 1326, Window and Dome Materials II, edited by P. Klocek (Bellingham, Washington, 1990) p. 144.
36. P. KLOCEK and J. T. HOGGINS, Proceedings of the Society of Photo-Optical Instrumentation Engineers, vol. 1760, Window and Dome Technologies and Materials III, edited by P. Klocek (Bellingham, Washington, 1992) p. 210.

Received 2 December 1992
and accepted 28 January 1994